

# Ecofriendly Synthesis of Copper Nanoparticles Using Coriander Seeds for Enhanced Adsorption Efficiency



Ayad Ali Disher<sup>1</sup>, Ali M.A. Al-Kufaishi<sup>3</sup> , Zainab Mohsen Najm<sup>4</sup>, Abbas Abdul Majeed Mohammed<sup>2</sup>, Lamia A. M. AlMashhedy<sup>1,\*</sup> , Baraa M. Alshelah<sup>5</sup> and Bashair H. Al Kinani<sup>1</sup>

<sup>1</sup>Chemistry Department, College of Science, University of Babylon, Iraq

<sup>2</sup>State Company for Gas Filling and Services, Hillah Gas Branch, Iraq

<sup>3</sup>Department of Medical Laboratory Techniques, College of Health and Medical Techniques, Al-Furat Al-Awsat Technical University, Kufa, Iraq 31003

<sup>4</sup>Department of Biochemistry, College of Medicine, University of Babylon, Iraq

<sup>5</sup>College of Dentistry, University of Akafeel, Al-Najaf, Iraq

## Abstract:

**Background:** Domestic gas cylinders are widely used in Iraq, and due to frequent usage and improper maintenance, organic sulfur group deposits accumulate. These deposits emit a pungent, harmful odor, and improper disposal methods, such as discarding cylinders in soil or rivers, pose environmental risks. Therefore, a need exists for an efficient and environmentally friendly method to remove these deposits.

**Objective:** This study aims to develop a green and safe method for removing organic sulfur group deposits from domestic gas cylinders using copper nanoparticles (CuNPs) synthesized through green chemistry.

**Methods:** Copper nanoparticles were synthesized using hot and cold aqueous extracts of coriander seeds (*Coriandrum sativum* L.) as reducing and stabilizing agents, with a 1mM aqueous solution of  $\text{CuSO}_4 \cdot 5\text{H}_2\text{O}$ . The formation of CuNPs was confirmed by color change and UV-visible scanning, showing an absorption peak in the 400-500 nm range. Optimization of temperature, time, pH, concentration of copper sulfate pentahydrate, and reactant mixing ratios was performed to achieve the most effective CuNPs production. The adsorption of organic sulfide groups, the main contaminants in gas cylinder sediments, onto the CuNPs surface was carried out using column chromatography and surface adsorption techniques.

**Results:** The optimal conditions for CuNPs synthesis were 1 mM copper sulfate pentahydrate, 70 °C, pH 9, reaction time of 60 minutes, and the ratio of extract to Copper Sulfate pentahydrate was observed at 20:80 mL. The CuNPs exhibited a high adsorption rate (90%) for organic sulfide groups, effectively removing these contaminants from gas cylinder sediments.

**Conclusion:** The large surface area of CuNPs enabled efficient separation, providing a green, rapid, and environmentally friendly solution for treating hazardous deposits in domestic gas cylinders, making them safe for disposal or reuse.

**Keywords:** Organic sulfide, Domestic gas cylinder, Copper nanoparticles, *Coriandrum sativum* L. (*C. sativum*), UV-visible, X-ray Diffraction and scanning electron microscope (SEM), Column chromatography and surface adsorption.

© 2025 The Author(s). Published by Bentham Open.

This is an open access article distributed under the terms of the Creative Commons Attribution 4.0 International Public License (CC-BY 4.0), a copy of which is available at: <https://creativecommons.org/licenses/by/4.0/legalcode>. This license permits unrestricted use, distribution, and reproduction in any medium, provided the original author and source are credited.



Received: December 13, 2024

Revised: March 02, 2025

Accepted: March 11, 2025

Published: April 23, 2025



Send Orders for Reprints to  
[reprints@benthamscience.net](mailto:reprints@benthamscience.net)

\*Address correspondence to this author at the Chemistry Department, College of Science, University of Babylon, Iraq; E-mail: [lamiaabdulmajeed@gmail.com](mailto:lamiaabdulmajeed@gmail.com)

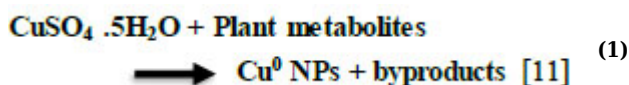
Cite as: Disher A, Al-Kufaishi A, Najm Z, Mohammed A, AlMashhedy L, Alshelah B, Al Kinani B. Ecofriendly Synthesis of Copper Nanoparticles Using Coriander Seeds for Enhanced Adsorption Efficiency. Open Biotechnol J, 2025; 19: e18740707373773. <http://dx.doi.org/10.2174/0118740707373773250411071011>

## 1. INTRODUCTION

*Coriandrum sativum* L. seed extracts were chosen in the present study because vitamin and mineral contents, including calcium, phosphorus, iron, carotene, riboflavin, thiamine, and niacin, also contain sodium, oxalic acid, and antioxidants [1]. Techniques involving reduction using seed plant (coriander) extracts are considered green synthesis methods [2]. Coriander plants belong to the family Apiaceae and contain several components, with the most important being fatty oil and essential oil. Coriander is also used as a medicinal agent to prevent convulsions, anxiety, insomnia, and loss of appetite. Coriander seeds, which are beneficial to health, are traditionally known for their anti-diabetic properties and their ability to reduce cholesterol levels [3]. The scientific classification of coriander is as follows: Kingdom: Plantae; Unranked: Angiosperms, Eudicots, Asterids; Order: Apiales; Family: Apiaceae; Genus: *Coriandrum*; Species: *C. sativum*; and the binomial name is *Coriandrum sativum* L [4].

Nanotechnology is one of the branches of science and the most active areas of research in modern materials science. Nanoparticles are usually defined as particles with at least one dimension in the range of 1 to 100 nm [5]. Nanotechnology has attracted many researchers from Different fields such as biotechnology, physics, material sciences, chemistry, engineering, and medicine [6]. New techniques for producing nanoparticles aim to use more affordable reagents, be environmentally friendly, and involve less severe reaction conditions. Copper nanoparticles have attracted scientific interest due to their potential antibacterial and anti-inflammatory properties [7, 8].

Research has shown that biomolecules such as flavonoids, proteins, and phenols not only aid in reducing particles to a nanosize but also play a crucial role in capping the nanoparticles [9]. Metal nanoparticles with antibacterial properties can be attached and coated onto various surfaces, opening up potential uses in various fields. Their antibacterial effect is attributed to their small size and high surface area-to-volume ratio, allowing for close interaction with microbial membranes [10]. Copper nanoparticles are produced from plant extracts, as depicted in Eq. (1).



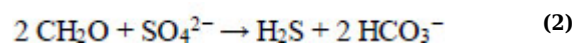
Catalytic applications of Cu-NPs synthesized from plant extracts are essential commodities in most industries, especially the chemical industries. Nano-catalysts are found to exhibit high specific surface area and surface energy, which ultimately promote their catalytic properties [12].

Nano-catalysts offer greater benefits compared to other catalysts due to their ability to enhance reaction selectivity at lower temperatures, reduce side reactions, exhibit high rates of recycling, and enable efficient recovery of energy. The application of nanocatalysts has garnered significant interest in various fields, including green chemistry, environmental remediation, solar cells, and medicine, as well as in industries such as dye, textile, and water treatment [13, 14].

An important means suggested to conquer the challenges arising from water contaminations and associated diseases is through wastewater treatment with nanoparticles because the traditional methods adopted in wastewater treatment cannot remove water pollutants [15].

Likewise, biogenic Cu-NPs were found to display potential photocatalytic activity useful for the degradation of azo dyes when adopted for the treatment of textile effluent. This activity was linked with the functional groups present in the extract used as reducing agents [16].

Organic sulfide is found widely in the environment due to human activities, such as tanning, chemical manufacturing, food processing, and the petrochemical industry. Sediments containing thiophene, an organic sulfide compound, is a major issue for gas-filling plants as they accumulate on the top of gas cylinders, leading to nozzle blockages, reduced efficiency, and potential explosions. These sediments are often disposed of in sewage water and rivers. Additionally, sulfate-reducing bacteria (SRB) use organic compounds as a carbon and energy source and utilize sulfate as the terminal electron acceptor for hydrogen sulfide production ( $\text{H}_2\text{S}$ ) and bicarbonate under anaerobic conditions, as shown in the Eq. (2) below [17]:



Therefore, besides organic compounds and sulfate, sulfide is also ubiquitous in these types of wastewater. The organic and sulfide /sulfate contamination is a typical corrosive, odorous pollutant and toxic to human health and living organisms, especially in anoxic sulfate-rich environment. Additionally, hydrogen sulfide is a gaseous molecule that accumulates in the environment from geothermal and

anthropogenic sources. It exists naturally in crude petroleum, natural gas, hot springs, and foods, also produced in large quantities in industrial activities and places such as petroleum/natural gas drilling and refining [18].

The wastewater must undergo treatment to eliminate harmful substances before being released into the environment. Sulfide can lead to the inhibition of the cytochrome oxidase enzyme system, causing a reduction in the use of oxygen by the cells. The buildup of lactic acid due to anaerobic metabolism results in an imbalance in the acid-base levels. The disruption of oxidative metabolism particularly affects the nervous system and cardiac tissues, often leading to respiratory arrest and, consequently, death. Additionally, hydrogen sulfide irritates the skin, eyes, mucous membranes, and respiratory tract. Pulmonary effects may become evident as late as 72 hours after exposure [19].

This research aims to remove organic sulfide present in sediment commonly found in gas cylinders and transform it from hazardous and toxic compounds to environmentally friendly substances before releasing them into wastewater or rivers. Furthermore, the study seeks to advocate for sustainable green chemistry and generate nanoparticles from medicinal plants to safeguard the environment with minimal expense from chemical waste.

## 2. MATERIALS AND METHODS

### 2.1. Preparation of Copper Nanoparticles

The Coriander *Sativum* seeds were gathered from the Iraqi local market. After thorough washing in deionized water, the seeds were allowed to air dry at room temperature. The seeds were lightly ground. Then, stored in a tightly sealed container. To prepare the hot extract, twenty grams of coarsely ground Coriander seeds were extracted by 100 ml of distilled water at 60 °C for 1 hour, then centrifuged at 3000 rpm for 15 min, and the supernatant was used as a colloidal solution to prepare the nanoparticles.

The Copper nanoparticles were prepared by adding 20 ml of aqueous extract of *C. Sativum* to 80 ml of 1 mM of  $\text{CuSO}_4 \cdot 5\text{H}_2\text{O}$  and heated with a stirrer at 70 °C for 60 min. The color change indicates the synthesis of copper nanoparticles.

To study the optimum factors for Copper nanoparticles synthesis, the experiments were carried out in different conditions such as the Copper ion concentration (0.5, 1, 2 and 2.5 mM), pH (3, 6, 7, 9, and 12), temperature (40 °C, 50 °C, 60 °C, 70 °C and 80 °C), time of reaction (10, 15, 30, 40, 60 min) and the ratio of *C. Sativum* extract to Copper sulfate pentahydrate (10:90, 20:80 and 30:70). The effect of these parameters on the synthesis of copper nanoparticles was detected by UV-Vis spectrophotometer.

## 2.2. Characterization of Copper Nanoparticles

### 2.2.1. By Color Change

The color change from dark brown to slight brown in aqueous extract indicates that the copper nanoparticles (CuNPs) were synthesized.

### 2.2.2. UV-visible Spectral Analysis

The reduction of copper ions ( $\text{Cu}^{2+}$ ) to copper nanoparticles ( $\text{Cu}^0$ ) was identified spectrometrically by a double-beam UV-Vis spectrophotometer (PG-303 UV) at various wavelengths (400-500 nm).

### 2.2.3. Atomic Absorption Spectrophotometer (AAS)

The rate of conversion of the  $\text{Cu}^{2+}$  ions to the  $\text{Cu}^0$  was analyzed by AAS (atomic absorption spectrophotometer (AA-6300 SHIMADZU)). This method provides a good indicator for the synthesis of (CuNPs)

### 2.2.4. X-Ray Diffraction (XRD)

The copper nanoparticles produced were spun at a speed of 15,000 rpm for 30 minutes, and the particles were gathered. The CuNPs were rinsed with distilled water to eliminate impurities and then dried to form a powder. An X-ray diffraction analysis was conducted using the Shimadzu X-ray diffractometer XRD-6000 AS (3K. NOPC) to identify the crystalline structure of the metal nanoparticles.

### 2.2.5. Scanning Electron Microscope (SEM)

Copper nanoparticles were meticulously deposited onto a glass cover slip and allowed to dry. This same cover slip was utilized for the scanning electron microscopy (SEM) analysis.

The SEM, or Scanning Electron Microscope, uses a beam of electrons to scan a sample in a raster pattern to create images. When the electrons interact with the atoms in the sample, they produce signals containing information about the sample's surface structure and composition. The INSPECT S50 FEI company conducted the SEM measurements.

### 2.2.6. Surface Adsorption and Column Chromatography of Sediments of Gas Domestic Gas Cylinder

The researchers selected sediments of domestic gas cylinders containing thiophene (an organic sulfide) for investigating the adsorption capacity of CuNPs. The experimental results were documented using a UV-Vis spectrophotometer configured at 225-250 nm [20]. CuNPs were synthesized and introduced into 100  $\text{cm}^3$  of sediment solutions. The solutions were periodically agitated in the dark using a shaker for 1 hour. The absorbance at the maximum absorption wavelength was analyzed before and after the adsorption process.

Batch adsorption testing was used to determine the removal percentage (R%) of organic sulfide on CuNPs. This involved placing 50, 100, 200 ppm of CuNPs with 100  $\text{cm}^3$  serial solutions of 0.1-0.5g  $\text{cm}^{-3}$  of sediments in separate conical flasks. The CuNPs containing sediments were shaken nicely at 100 rpm on a shaker at 25 °C in the dark until they reached equilibrium. The concentration of sediments was determined using a UV-vis spectrophotometer (PG UV-visible spectrometer). The sediment removal percentage and the adsorption quantity of the sediments adsorbed per unit mass of adsorbent were calculated using a specific Eq. (3) [21].

$$\% R = (C_0 - C_t/C_0) \times 100 \% \quad (3)$$

The initial sediment concentration ( $C_0$ ) is the amount of sediments in solution ( $\text{mg dm}^{-3}$ ) before adsorption takes place. After a given time ( $t$ ), the sediment concentration ( $C_t$ ) will change due to adsorption.

A column was filled with cellulose as a stationary phase and saturated with a solution of sediments (containing sulfide group as a contaminate). Copper nanoparticles of *Coriander sativum* were added as eluent, while the eluent was passed through the column, different components of the sample were carried at different rates, resulting in the separation of components, the eluate (the solvent leaving the column) was collected in separate fractions using clean vessels till the clarity of colour solutions achieved. The collected fractions were analyzed to identify the presence of different components by using spectrophotometry.

### 3. RESULTS AND DISCUSSION

#### 3.1. Characterization of Copper Nanoparticles

##### 3.1.1. By Color Change

The progress in the reduction of copper ions to copper nanoparticles using the hot seed extracts was indicated by the increased intensity of surface Plasmon absorption peak observed at 420-430 nm. Metal nanoparticles exhibit various colors in solution cause to their optical properties [22, 23]. The formation of CuNPs was primarily well known by the color change from dark brown to slight brown in aqueous extract (Figs. 1-2).

##### 3.1.2. Effect of Copper Sulfate Pentahydrate Concentration

The concentration of copper sulfate pentahydrate is considered as an important effect in the synthesis of

copper nanoparticles using *Coriandrum sativum* L. The surface plasmon absorption band characteristic was observed for the copper ion concentration nanoparticles synthesized 1mM  $\text{CuSO}_4 \cdot 5\text{H}_2\text{O}$ . The absorption was increased with increasing copper ion concentration from 0.5 mM, 1 mM, 2 mM, and 2.5 mM concentration were the optimum conditions for CuNPs shown in Fig. (3). Also, we have noticed that increasing the  $\text{CuSO}_4 \cdot 5\text{H}_2\text{O}$  concentration leads to a distortion of the peak, which is moving away from the  $\lambda$  maximum for copper nanoparticles [24, 25].

This result highlights the importance of the initial copper ion concentration in the synthesis process and its direct impact on the characteristics of the resulting copper nanoparticles.

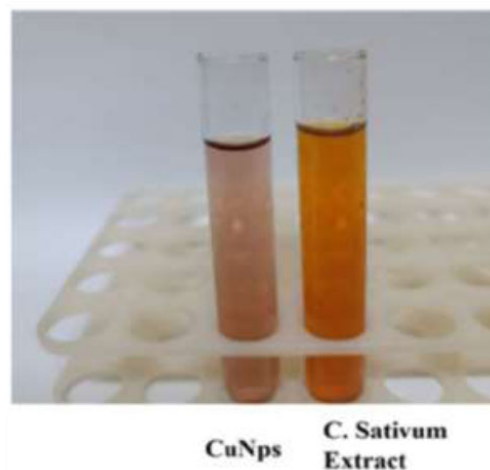


**Fig. (1).** Copper nanoparticles prepared from hot coriander sativum extracts.

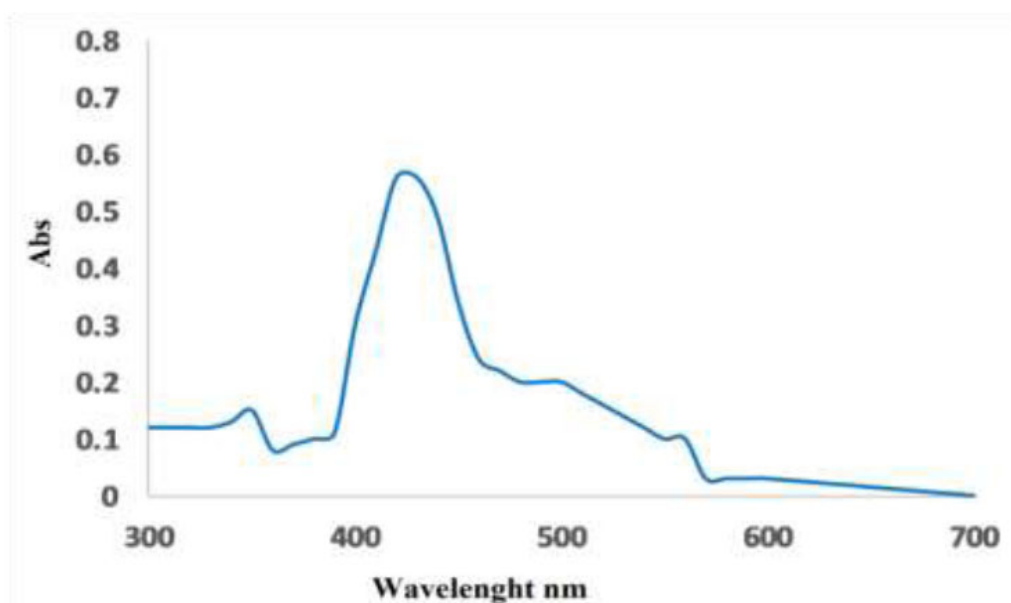


**Fig. (2).** UV- vis spectrum for copper nanoparticles prepared from hot coriander sativum extract.

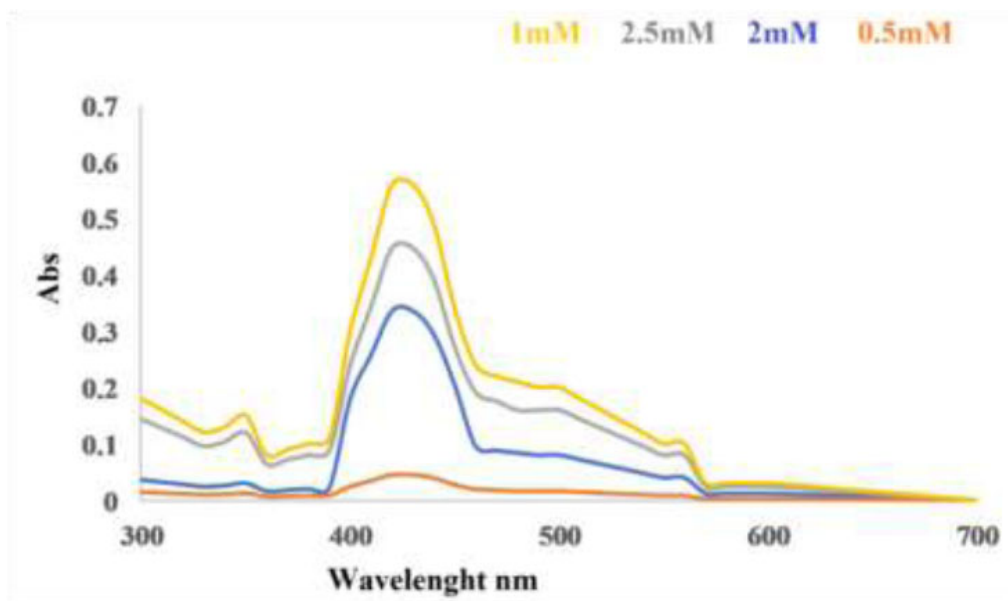


**Fig. (3).** Effect of copper sulfate pentahydrate concentration on synthesis of copper nanoparticles using hot extract.

### 3.1.3. Effect of pH

The synthesis of copper nanoparticles was investigated to determine the impact of pH within a range of 3 to 12, as depicted in Fig. (4). The surface plasmon absorbance of copper colloids was obtained for all pH. The aggregation of the smallest copper nanoparticles under optimal conditions leads to a red-shift in the surface plasmon resonance, affecting the absorbance properties of the colloidal solution [26].

The highest absorption in the UV-visible absorption spectra occurs at pH 9 when forming CuNPs from both hot and cold extracts. The synthesis of large nanoparticle size with a broadening surface plasmon resonance band may be due to different factors such as particle shape, size, and spatial distribution within a template. Moreover, the shape distribution of nanoparticles, ranging from cylinder to spheres, can notably affect the plasmon band broadening [27].

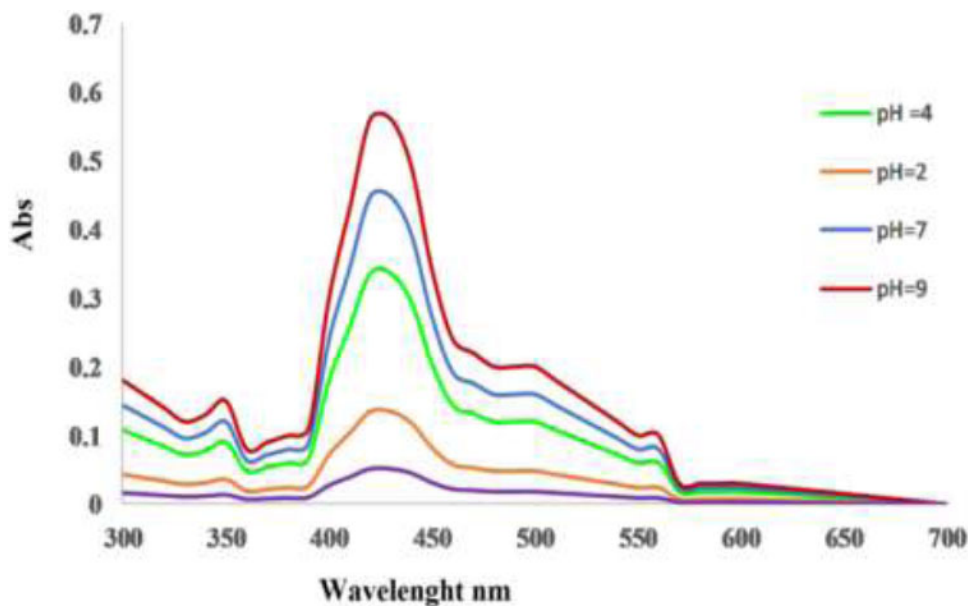


**Fig. (4).** pH Effect of hot nanoparticles.



Additionally, the spectral response of nanoparticles is affected by the size reduction, where smaller particles exhibit increased surface contributions to the localized surface plasmon resonance linewidth due to the quantum confinement of electrons [28].

Arya. *et al.* [29] and Caroling. *et al.* [30] described how pH affects the shape and size of CuNPs, noting that a large number of particles form in alkaline pH, while acidic pH leads to increased aggregation of nuclei rather than particle formation. The study suggests that alkaline pH is better for synthesizing copper nanoparticles. These findings emphasize the relationship between metal nanoparticle properties and their impact on the formation of larger nanoparticles with extended surface plasmon resonance bands [24].

### 3.1.4. Effect of Temperature

In the process of nanoparticle formation, temperature is a critical factor that influences the nucleation process. According to Fig. (5), the absorbance rises as the temperature climbs from 60 °C to 70 °C, but then declines at higher temperatures. Lee HJ *et al.* [31] discovered that as the reaction temperature increased from 25 °C to 95 °C, both the synthesis rate and the conversion to copper nanoparticles also increased. Similarly, Amjad R. *et al.* [24] noted that the optimal formation of CuNPs occurred at 70 °C. The green synthesis of CuNPs demonstrated the effect of temperature on production; at low temperatures, production was reduced by half, whereas at higher temperatures, the reduction of  $\text{Cu}^{2+}$  ions to form small nanoparticles was accelerated, although aggregates were also formed [30].

At elevated temperatures, the rate of reduction was higher because copper ions were used up in forming nuclei, while the secondary reduction halted on the surface of the nuclei. According to Lee, HJ. *et al.* [31], the effect of temperature on the rate of copper nanoparticle composition rises as the temperature reaches 60-70 °C.

### 3.1.5. Effect of Reaction Time

Fig. (6) show that the absorbance spectrum gradually increased as the reaction time increased, leading to a corresponding increase in color intensity during the incubation period. The maximum absorbance was observed after 60 minutes of reaction time, indicating a direct relationship between reaction time, absorbance spectrum, color intensity, and the formation of CuNPs, which is essential for comprehending the kinetics of the process. Our research indicates that the absorbance spectrum and color intensity gradually increase with longer reaction times, peaking at 60 minutes, demonstrating a direct correlation between reaction duration and these optical properties. Moreover, the peak intensity of the surface plasmon resonance indicates the formation of CuNPs and increases with longer incubation periods, highlighting the relationship between reaction time and CuNPs generation. This changing process emphasizes the importance of monitoring and understanding the kinetics of these reactions to achieve the best results, as longer incubation results in increased absorbance, color intensity, and CuNPs formation, demonstrating the complex interaction between reaction time and product properties [32].

Lee *et al.* [33] found that CuNPs formed within 24 hours of incubation, while another study demonstrated that the ideal reaction time for completion was 30 minutes [34].

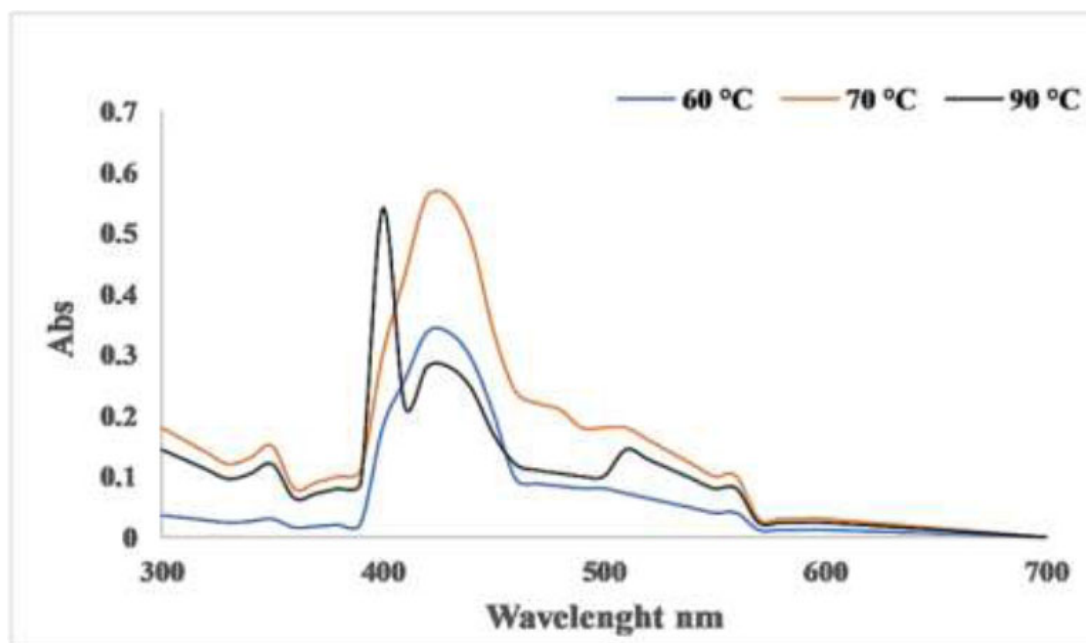
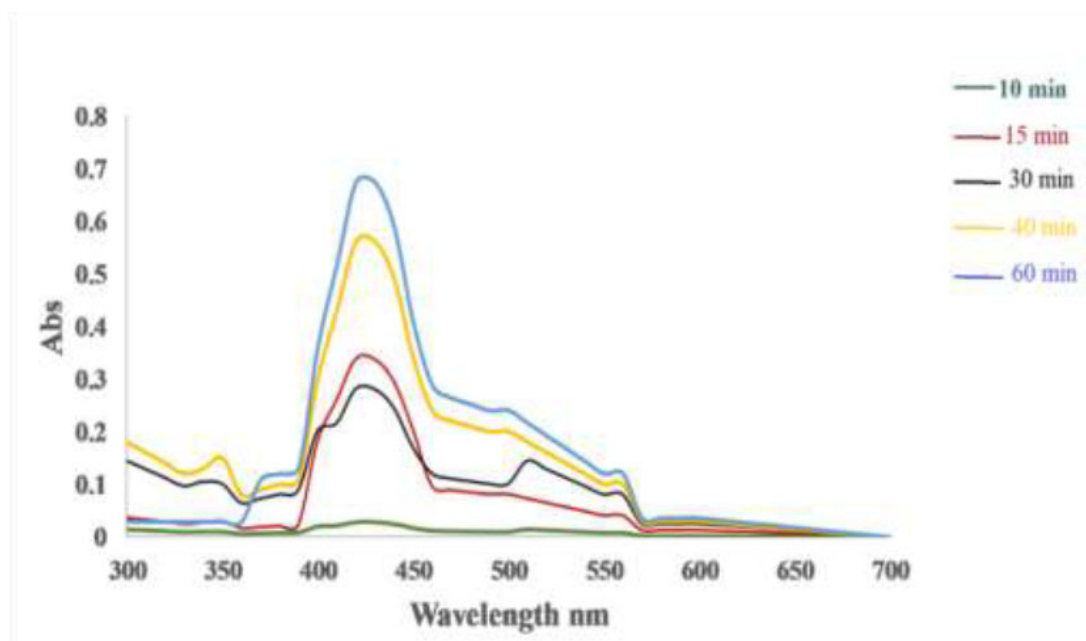


Fig. (5). Effect of different reaction temperature for hot CuNPs.



**Fig. (6).** Reaction time for synthesis of CuNPs from hot extract.

### 3.1.6. The Ratio of Copper Sulfate Pentahydrate and *Coriandrum sativum* L. Extract

The study was conducted on the impact of extract concentration in the mixed solution on the biosynthesis of copper nanoparticles. The variance of extract concentration

in the mixed solution was obtained by adjusting the volume of the added extract solution at different volumes. The optimization of extract to Copper Sulfate pentahydrate ratio was observed at 20:80 mL for the aqueous extract as shown in Fig. (7).

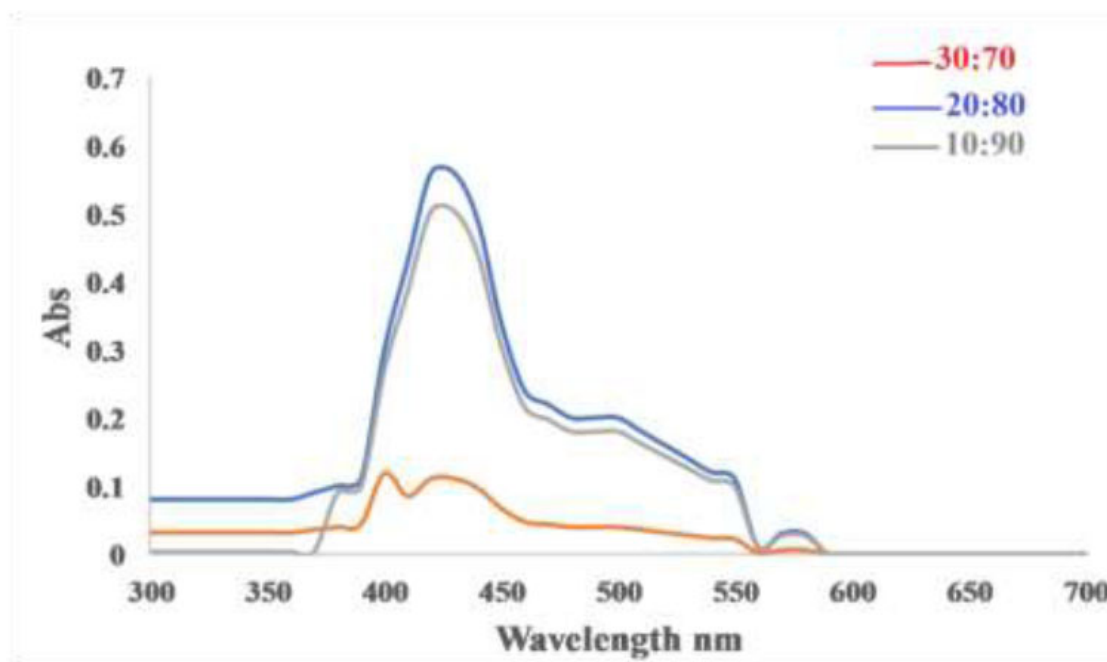


**Fig. (7).** Effect the ratio of *coriandrum sativum* L. hot extract (ml):  $\text{CuSO}_4 \cdot 5\text{H}_2\text{O}$  (ml).

### 3.1.7. Map of Copper Nano particulars

The image map in Fig. (8) reflects the particular copper has a yellow color point.

The nanoparticle of copper is represented by the yellow color points on an image map, which may be due to the fluorescent properties of copper nanoclusters (CuNPs). These particles are extremely small nanoclusters with strong fluorescence, making them well-suited for bioimaging applications, such as optical imaging technology commonly employed in biomedicine research. Thus, the yellow colour points on the image map could potentially indicate the

presence and specific attributes of copper nanoclusters at a microscopic level [34-36].

### 3.1.8. X-Ray Diffraction Studies (XRD)

The synthesis of CuNPs using green methods was also confirmed by X-ray diffraction (XRD), as depicted in Fig. (9). The Debye Scherrer's formula was employed to calculate the average diameter of the copper nanoparticles in the 30-90nm range, using the Full Width at Half Maximum (FWHM) obtained from the diffraction peaks:  $D = 0.89\lambda / \beta \cos\theta$ .

Image map in Figure (14 a and b) reflects the particular copper has a yellow color points.



Fig. (8). Map image of CuNPs.

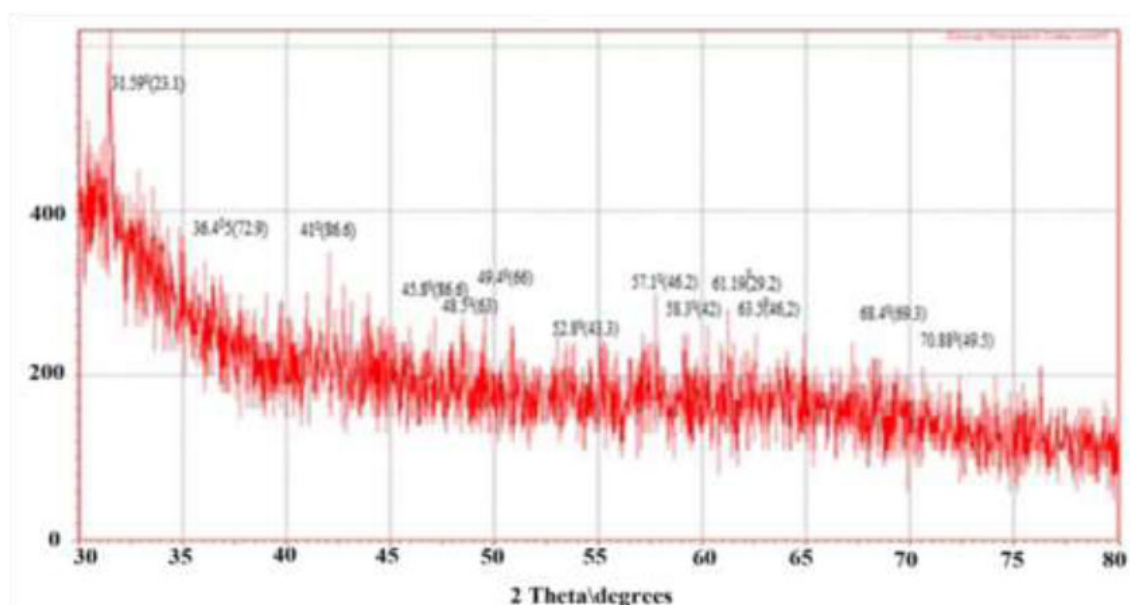


Fig. (9). X-Ray pattern of CuNPs hot aqueous extract.



The mean grain size is denoted by  $D$ , while  $\beta$  represents the FWHM of the diffraction peaks, and  $\theta$  stands for the diffraction angle, where  $\lambda$  is the wavelength of the copper target. Consequently, XRD is a frequently employed technique for determining the chemical composition and crystal structure of a material [37]. The apparent peak broadening and interference may be attributed to the impact of nanoscale particles and the existence of various crystalline biological macromolecules in plant extract. In the results observed, the difference in preparation conditions between the hot and cold extracts has led to a noticeable disparity in the quality of the X-ray diffraction (XRD) patterns obtained. Preparation using the hot extract likely promotes the formation of more uniform and crystalline nanoparticles, reflected in the sharp and well-defined peaks in the diffraction pattern. These sharp peaks indicate a high degree of crystallinity and purity of the particles.

In contrast, the noise observed in the diffraction pattern of the cold extract may suggest the presence of smaller or heterogeneous crystals or even a more random size distribution. This results in a less distinct diffraction pattern, where the peaks are less sharp and perhaps more broadened, indicating poor crystallinity or a higher presence of amorphous material.

### 3.1.9. Scanning Electron Microscope (SEM)

The result in (Fig. 10) shows the SEM images displayed various shapes of CuNPs, with particle sizes ranging from 40–76 nm for the hot extract and 32–68 nm for the cold extract. The synthesis of copper nanoparticles using plant extract is attributed to the electrostatic interactions and hydrogen bonds formed by the bio-organic capping molecules.

### 3.1.10. Energy Dispersive X-ray Crystallography (EDX)

The quantitative and qualitative analysis of elements may be concerned with the formation of copper nanoparticles. The identified EDX analysis Fig. (11). Due to the Surface Plasmon Resonance, the copper nanoparticle shows

the absorption peaks of higher counts [32]. The strongest principal sharp signal was observed at 1 keV for copper, and some of the weak peaks for C, O, Al, Ca, S, and H was found in the hot extract, and C, O, Al, Ca, S, and H were found in the cold extract. The presence of the weak signal may possibly be due to the biomolecules that are bound to the surface of CuNPs [6, 29].

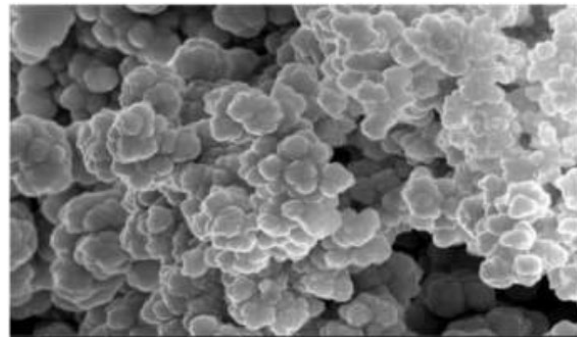


**Fig. (10).** SEM micrograph of CuNPs for hot extract.

### 3.1.11. Flame Atomic Absorption Spectrophotometer (AAS)

It is feasible to measure the transformation of copper ions into copper particles using the AAS technique. This method demonstrates a gradual reduction in the concentration of copper ions until they completely vanish, suggesting the complete conversion of copper ions ( $\text{Cu}^{+2}$ ) into copper ( $\text{Cu}^0$ ) and the formation of nanoparticles. At the start, standard solutions of  $\text{CuSO}_4 \cdot 5\text{H}_2\text{O}$  at 50, 100, and 200 ppm were prepared and analyzed immediately. Fig. (12) shows the rate of decrease in the concentration of copper ions (200 ppm at 0, 15, 30, and 45 min respectively). This data reflects the conversion of copper ions into copper particles. The observed decrease in ion concentration over time indicates that as the reaction progresses, more copper ions are being reduced and converted into nanoparticles [21].

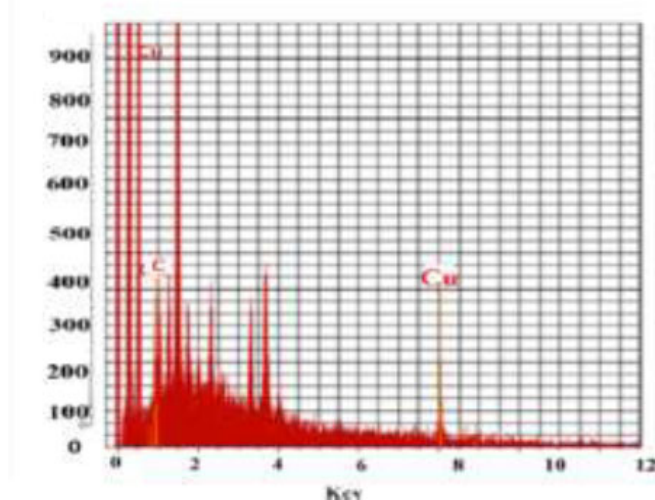


**Fig. (11).** EDX analysis of CuNPs.

ELAN Series	Atomic No.	Wt%
C	6	4.2
O	8	4.6
Al	13	1.18
Ca	20	0.09
Cu	29	73.3
S	16	0.24
H	1	3.5

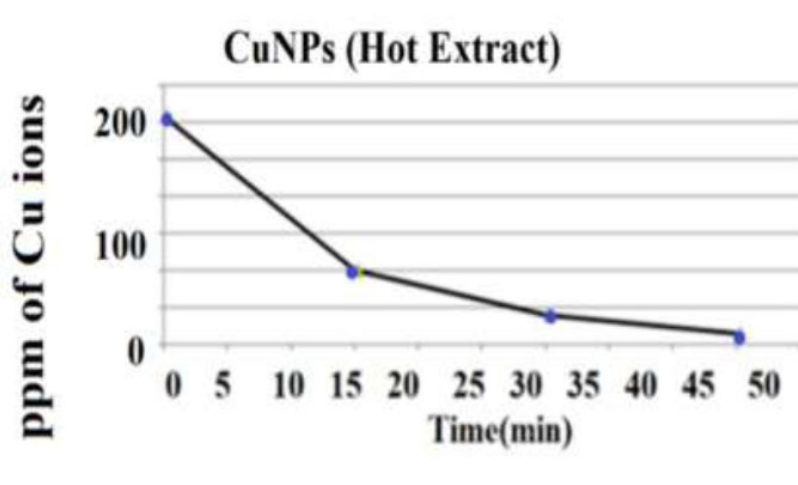


**Fig. (12).** Atomic absorption analysis of copper sulfate pentahydrate (ppm) with reaction time (min) using coriandrum sativum aqueous extract to synthesis of copper nanoparticles.

### 3.1.12. Surface Adsorption and Column Chromatography for Sediments of Domestic Gas Cylinder

In this study, we investigated the removal of the sulfide group from the sediments. The UV-visible spectrum of the sulfide group in thiophene appears at 220–250 nm. The UV-visible spectra of the sediments are shown in Fig. (16). After adsorption on the surface of CuNPs, the spectra indicate the absence of these peaks. The effectiveness of the created CuNPs in eliminating the organic sulfide group was evaluated, and the increase in CuNPs dosage led to a rise in

the percentage of organo-sulfide adsorption. This was due to the greater probability of the organic sulfide coming into contact with the active sites of the CuNPs, which increases with the rise in the quantity of the adsorbent. However, the adsorption capacity for organic sulfide increased as the dosage of CuNPs increased, as illustrated in Fig. (13). This result may be due to the adsorption capacity, which is related to the quantity of adsorbent used. The current investigation examined the efficacy of nanoparticles in removing organic sulfide in sediments of gas domestic cylinder.

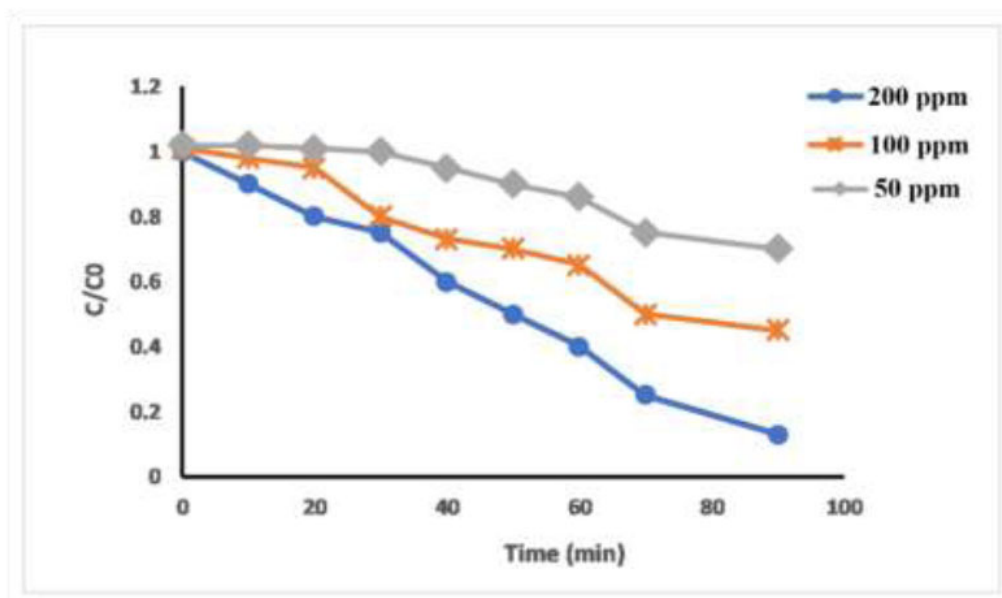


**Fig. (13).** Removal of sediments with different concentrations of copper nanoparticles by using surface adsorption method. Where  $C_0$  is the sediment concentration at the beginning of adsorption;  $C$  is the concentration after degradation.

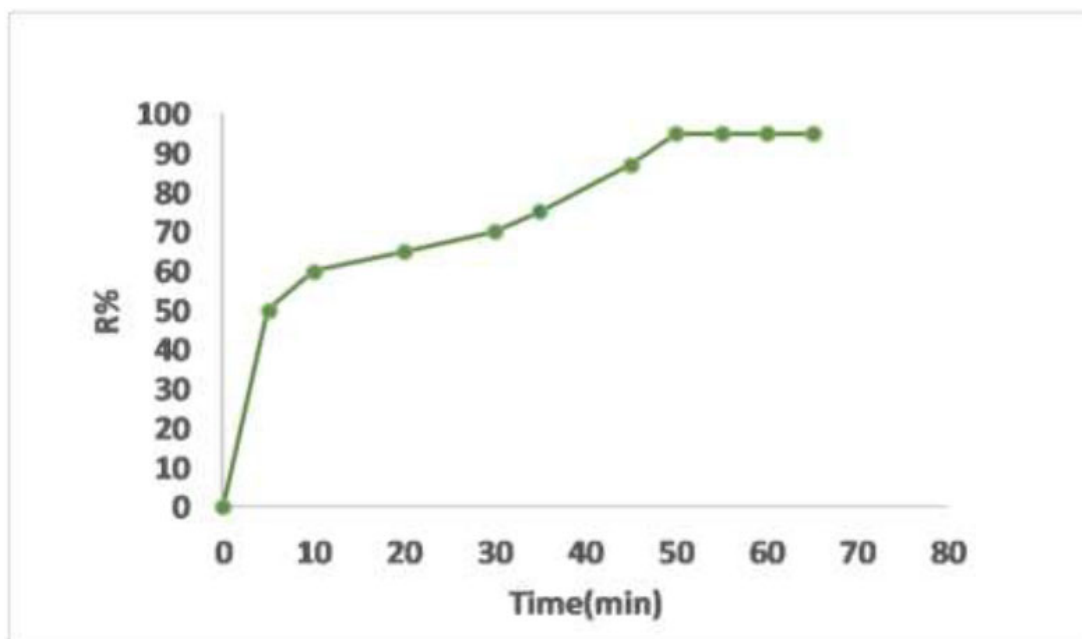


**Fig. (14).** Illustrates the impact of time on the percentage of organic sulfide removal from sediments. The initial concentration is  $0.5 \text{ g cm}^{-3}$ , and the adsorbent dosage is  $0.1 \text{ g}$  in  $100 \text{ cm}^3$  of organic sulfide solutions. The shaking rate is consistently maintained at  $100 \text{ rpm}$ , and the temperature is set at  $25^\circ \text{C}$ .

The initial stages explained a rapid advancement in the adsorption of organic sulfide onto nanoparticles, but the rate gradually diminished, eventually reaching equilibrium after 50 minutes, as depicted in Fig. (14). Since all the adsorbent sites were initially unoccupied, the adsorption rate underwent rapid changes. Subsequently, the adsorption rate decreased due to the reduction in the number of vacant adsorbent sites and the sediment concentration. The decrease in the adsorption rate indicates the likely formation of a monolayer of organic sulfide on the adsorbent surface. Consequently, after reaching equilibrium, the insufficiency of available active sites necessitates further uptake [38].

The adsorption of organic molecules is typically influenced by multiple mechanisms. Therefore, it is important to gain a deep understanding of the complex adsorption mechanisms involved in the uptake of pollutants to determine the predominant adsorption pathway, particularly when organic pollutants are present as a mixture in wastewater feeds. The effectiveness of nanoparticles in adsorbing organic compounds is significantly enhanced by surface functionalization. Functional groups such as Alkaloids, flavonoids, *etc.* in natural compounds play a crucial role in improving surface properties such as specific area, charge density, porosity, and hydrophilicity while also providing additional sorption sites for organic molecules [39].

In Fig. (15), the UV-vis spectra were utilized to measure the concentrations of organic sulfide both before and after adsorption. It was observed that the organic sulfide was eliminated from the aqueous solution and adsorbed

onto the nanoparticles. Following adsorption, minimal absorption bands for organic sulfide were detected in the sediment solution through UV-vis spectra. This phenomenon could be attributed to the electrostatic attraction between the nanoparticles and organic sulfide, resulting in the capture of sediments on the nanoparticles.

Also, the results in Fig. (16) show the sulfide and CuNPs peaks. The disappearance of the peaks gives an indication of the withdrawing of the sulfide group by the nanoparticles and perhaps the formation of a new compound, leaving environmentally friendly materials that can be safely handled.

Nanoparticles possess valuable characteristics such as a high specific surface area, active sorption sites, solubility, efficiency, and fractal dimension. They also have a short intraparticle diffusion distance, a well-defined chemical composition, small particle size, and adjustable pore size compared to their bulk counterparts, which contribute to their effective sorption, especially chemical activity and fine grain size. The high surface area and active sorption sites in nanoparticles are attributed to their high surface energy and size-dependent surface structure at the nanoscale. Nanoparticles demonstrate the highest efficiency in adsorbing organic and inorganic pollutants, and their selectivity towards contaminants can be enhanced through surface functionalization [40, 41]. The strong adsorption strength, greater surface area, and chemical stability of nanomaterial adsorbents make them promising tools in the removal of hazardous contaminants from industrial effluents, which highlights their use in wastewater treatment.

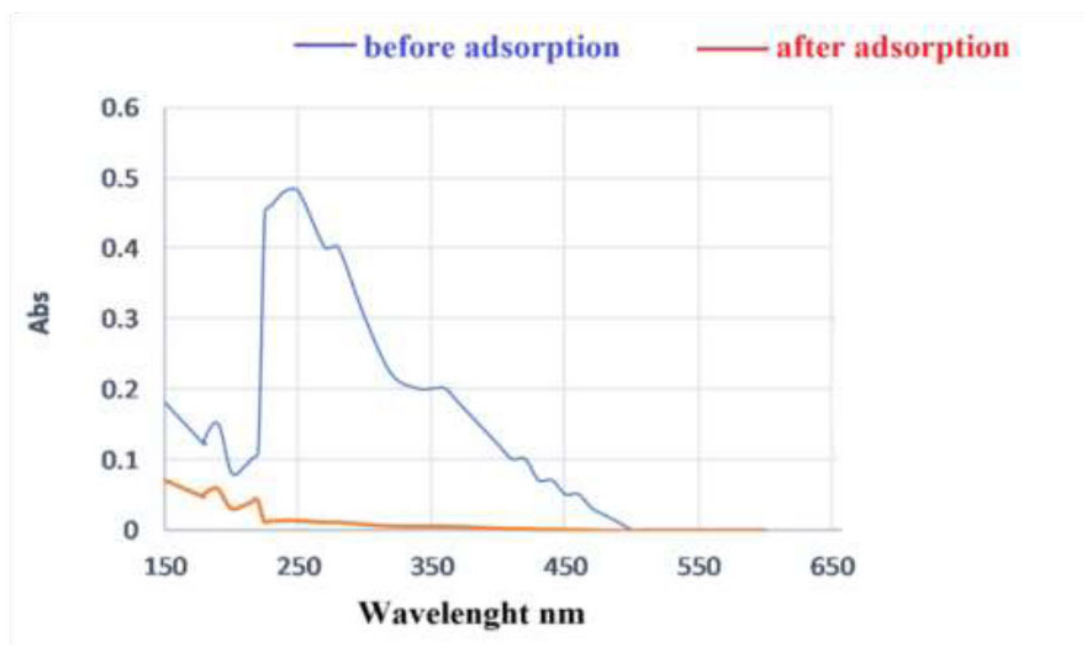


**Fig. (15).** A UV-vis spectra of sediments solutions before and after adsorption on the CuNPs adsorbent.

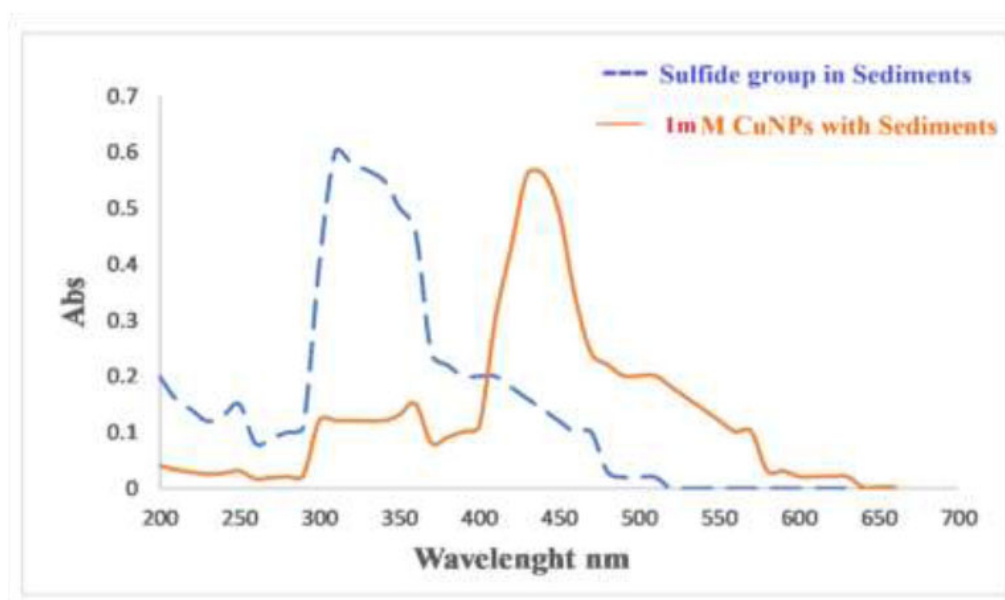


**Fig. (16).** UV-visible of sediments adsorption before and after mixing with CuNPs using column chromatography.

## CONCLUSION

The optimal conditions for the synthesis of copper nanoparticles were as follows: a copper sulfate pentahydrate concentration of 1 mM, temperature of 70 °C, pH of 9, incubation time of 60 minutes, and an extract to copper sulfate pentahydrate ratio of 20:80 ml. UV-visible scanning showed qualitative formation of CuNPs and characteristic absorption peak in the range of 400-500 nm. These results

may be due to the phytochemical species in *Coriander sativum* extracts. The green synthesis of CuNPs is a simple, clean, eco-friendly, and nontoxic environmental method. The research demonstrated the ability of copper nanoparticles to adsorb pollutants such as the organic sulfide group and thus get rid of their toxicity by converting them into harmless compounds and converting the sediments as well into environmentally friendly materials. The unique



properties of copper nanoparticles, such as high surface energy and size-dependent surface structure, may account for this ability.

The utilization of copper salts in biosynthesizing copper nano catalysts further highlights the sustainable and effective nature of these nanoparticles, offering a viable alternative for removing the environmental pollutant and as a promising approach for removing sulfide groups in domestic gas cylinder sediments due to their adsorption potential.

## AUTHORS' CONTRIBUTIONS

The authors confirm their contribution to the paper as follows: A.A.D., A.A.M.M.: Study conception and design; B.H.A.K.: Data collection; A.M.A.A.K.: Data analysis or interpretation; B.M.A., Z.M.N.: Investigation; L.A.M.A.: Draft manuscript. All authors reviewed the results and approved the final version of the manuscript.

## ETHICS APPROVAL AND CONSENT TO PARTICIPATE

Not applicable.

## HUMAN AND ANIMAL RIGHTS

Not applicable.

## CONSENT FOR PUBLICATION

Not applicable.

## AVAILABILITY OF DATA AND MATERIALS

All the data and supporting information are provided within the article.

## FUNDING

None.

## CONFLICT OF INTEREST

The authors declared no conflict of interest, financial or otherwise.

## ACKNOWLEDGEMENTS

We would like to express our gratitude to all the researchers involved in this study for their valuable contributions and collaboration. No funding was received for this research. The work presented here is the result of our collective efforts and dedication.

## REFERENCES

- [1] Heidari B, Sajjadi SE, Minaian M. Effect of *Coriandrum sativum* hydroalcoholic extract and its essential oil on acetic acid- induced acute colitis in rats. *Avicenna J Phytomed* 2016; 6(2): 205-14. PMID: 27222834
- [2] Sathyavathi R, Krishna MB, Rao SV, Saritha R, Rao DN. Biosynthesis of silver nanoparticles using *Coriandrum sativum* leaf extract and their application in nonlinear optics. *Adv Sci Lett* 2010; 3(2): 138-43. <http://dx.doi.org/10.1166/asl.2010.1099>
- [3] Delaquis P, Stanich K, Girard B, Mazza G. Antimicrobial activity of individual and mixed fractions of dill, cilantro, coriander and eucalyptus essential oils. *Int J Food Microbiol* 2002; 74(1-2): 101-9.

- [http://dx.doi.org/10.1016/S0168-1605\(01\)00734-6](http://dx.doi.org/10.1016/S0168-1605(01)00734-6) PMID: 11929164
- [4] Burdock GA, Carabin IG. Safety assessment of coriander (*Coriandrum sativum* L.) essential oil as a food ingredient. *Food Chem Toxicol* 2009; 47(1): 22-34. <http://dx.doi.org/10.1016/j.fct.2008.11.006> PMID: 19032971
- [5] Szczygłowska P, Feliczak-Guzik A, Nowak I. Nanotechnology-general aspects: A chemical reduction approach to the synthesis of nanoparticles. *Molecules* 2023; 28(13): 4932. <http://dx.doi.org/10.3390/molecules28134932> PMID: 37446593
- [6] Yang G, Chai S, Xiong X, Zhang S, Yu L, Zhang P. Preparation and tribological properties of surface modified Cu nanoparticles. *Trans Nonferrous Met Soc China* 2012; 22(2): 366-72. [http://dx.doi.org/10.1016/S1003-6326\(11\)61185-0](http://dx.doi.org/10.1016/S1003-6326(11)61185-0)
- [7] Thakur S, Sharma S, Thakur S, Rai R. Green synthesis of copper nano-particles using *Asparagus adscendens* Roxb. Root and leaf extract and their antimicrobial activities. *Int J Curr Microbiol Appl Sci* 2018; 7(4): 683-94. <http://dx.doi.org/10.20546/ijcmas.2018.704.077>
- [8] Gupta D, Barwal I, Kaur P. Green synthesis of copper nanoparticles using medicinal plants and their biomedical applications: A review. *Mater Today Chem* 2022; 27: 101464. <http://dx.doi.org/10.1016/j.mtchem.2022.101464>
- [9] Ahmad N, Sharma S, Singh V N, Shamsi S F, Fatma A, Mehta B R. Biosynthesis of silver nanoparticles from *Desmodium triflorum*: A novel approach towards weed utilization. *Biotechnol Res Int* 2011; 2011(2090-3138): 454090.
- [10] Roy S, Rao K, Bhuvaneswari C, Giri A, Mangamoori LN. Phytochemical analysis of *Andrographis paniculata* extract and its antimicrobial activity. *World J Microbiol Biotechnol* 2010; 26(1): 85-91. <http://dx.doi.org/10.1007/s11274-009-0146-8>
- [11] Kuppusamy P, Yusoff MM, Maniam GP, Govindan N. Biosynthesis of metallic nanoparticles using plant derivatives and their new avenues in pharmacological applications - An updated report. *Saudi Pharm J* 2016; 24(4): 473-84. <http://dx.doi.org/10.1016/j.jsps.2014.11.013> PMID: 27330378
- [12] Atri A, Echabaane M, Bouzidi A, Harabi I, Soucase BM, Ben Chaâbane R. Green synthesis of copper oxide nanoparticles using *Ephedra Alata* plant extract and a study of their antifungal, antibacterial activity and photocatalytic performance under sunlight. *Heliyon* 2023; 9(2): e13484. <http://dx.doi.org/10.1016/j.heliyon.2023.e13484> PMID: 36816263
- [13] Antonio-Pérez A, Durán-Armenta LF, Pérez-Loredo MG, Ana Laura Torres-Huerta AL. Biosynthesis of copper nanoparticles with medicinal plants extracts: From extraction methods to applications. *Micromachines* 2023; 14(10): 1882.
- [14] Dobrucka R. Antioxidant and catalytic activity of biosynthesized CuO nanoparticles using extract of *Galeopsis herba*. *J Inorg Organomet Polym Mater* 2018; 28(3): 812-9. <http://dx.doi.org/10.1007/s10904-017-0750-2>
- [15] Natarajan B, Kannan P, Rather JA, Sheikh RA. Recent developments in metal nanoparticles functionalized nanocomposite adsorbents for heavy metals removal from wastewaters. *J Taiwan Inst Chem Eng* 2023; 147: 104942-2. <http://dx.doi.org/10.1016/j.jtice.2023.104942>
- [16] Saim AK, Adu PCO, Amankwah RK, Oppong MN, Darteh FK, Mamudu AW. Review of catalytic activities of biosynthesized metallic nanoparticles in wastewater treatment. *Environ Technol Rev* 2021; 10(1): 111-30. <http://dx.doi.org/10.1080/21622515.2021.1893831>
- [17] Kieu TQH, Nguyen TY, Do CL. Treatment of organic and sulfate/sulfide contaminated wastewater and bioelectricity generation by sulfate-reducing bioreactor coupling with sulfide-oxidizing fuel cell. *Molecules* 2023; 28(17): 6197. <http://dx.doi.org/10.3390/molecules28176197> PMID: 37687026
- [18] Kim KH, Jeon EC, Choi YJ, Koo YS. The emission characteristics and the related malodor intensities of gaseous reduced sulfur compounds (RSC) in a large industrial complex. *Atmos Environ* 2006; 40(24): 4478-90.



- <http://dx.doi.org/10.1016/j.atmosenv.2006.04.026>
- [19] Batterman S, Grant-Alfieri A, Seo SH. Low level exposure to hydrogen sulfide: A review of emissions, community exposure, health effects, and exposure guidelines. *Crit Rev Toxicol* 2023; 53(4): 244-95.  
<http://dx.doi.org/10.1080/10408444.2023.2229925> PMID: 37431804
- [20] Potratz S, Mishra A, Bäuerle P. Thiophene-based donor-acceptor co-oligomers by copper-catalyzed 1,3-dipolar cycloaddition. *Beilstein J Org Chem* 2012; 8(1): 683-92.  
<http://dx.doi.org/10.3762/bjoc.8.76> PMID: 23015814
- [21] Halbus AF, Athab ZH, Abbas AS, Khaleel AK, Wahhoodee SM, Atiyah AJ. Adsorption, photodegradation, and selective removal of reactive red 2 dye onto cuprous oxide nanoparticles. *Monatsh Chem* 2022; 153: 597-607.  
<http://dx.doi.org/10.1007/s00706-022-02955-3>
- [22] Hassan E, Gahlan AA, Gouda GA. Biosynthesis approach of copper nanoparticles, physicochemical characterization, cefixime wastewater treatment, and antibacterial activities. *BMC Chem* 2023; 17(1): 71.  
<http://dx.doi.org/10.1186/s13065-023-00982-7> PMID: 37424027
- [23] Jalab J, Abdelwahed W, Kitaz A, Al-Kayali R. Green synthesis of silver nanoparticles using aqueous extract of *Acacia cyanophylla* and its antibacterial activity. *Heliyon* 2021; 7(9): e08033.  
<http://dx.doi.org/10.1016/j.heliyon.2021.e08033> PMID: 34611564
- [24] Amjad R, Mubeen B, Ali SS, et al. Green synthesis and characterization of copper nanoparticles using *Fortunella margarita* leaves. *Polymers* 2021; 13(24): 4364.  
<http://dx.doi.org/10.3390/polym13244364> PMID: 34960915
- [25] Adewale Akintelu S, Kolawole Oyebamiji A, Charles Olugbeko S, Felix Latona D. Green chemistry approach towards the synthesis of copper nanoparticles and its potential applications as therapeutic agents and environmental control. *Curr Res Green Sustain Chem* 2021; 4: 100176.  
<http://dx.doi.org/10.1016/j.crgsc.2021.100176>
- [26] Ghosh SK, Rahman DS, Ali AL, Kalita A. Surface plasmon tunability and emission sensitivity of ultrasmall fluorescent copper nanoclusters. *Plasmonics* 2013; 8(3): 1457-68.  
<http://dx.doi.org/10.1007/s11468-013-9559-1>
- [27] Machida K, Adachi K. Particle shape inhomogeneity and plasmon-band broadening of solar-control LaB<sub>6</sub> nanoparticles. *J Appl Phys* 2015; 118(1): 013103.  
<http://dx.doi.org/10.1063/1.4923049>
- [28] Juvé V, Cardinal MF, Lombardi A, et al. Size-dependent surface plasmon resonance broadening in nonspherical nanoparticles: Single gold nanorods. *Nano Lett* 2013; 13(5): 2234-40.  
<http://dx.doi.org/10.1021/nl400777y> PMID: 23611370
- [29] Arya V. Living systems: Eco-friendly nano factories. *Dig J Nanomater Biostruct* 2010; 5(1): 9-21.
- [30] Kaur P, Thakur R, Chaudhury A. Biogenesis of copper nanoparticles using peel extract of *Punica granatum* and their antimicrobial activity against opportunistic pathogens. *Green Chem Lett Rev* 2016; 9(1): 33-8.  
<http://dx.doi.org/10.1080/17518253.2016.1141238>
- [31] Lee HJ, Song JY, Kim BS. Biological synthesis of copper nanoparticles using *Magnolia kobus* leaf extract and their antibacterial activity. *J Chem Technol Biotechnol* 2013; 88(11): 1971-7.  
<http://dx.doi.org/10.1002/jctb.4052>
- [32] Biegel M, Schikarski T, Cardenas Lopez P, et al. Efficient quenching sheds light on early stages of gold nanoparticle formation. *RSC Advances* 2023; 13(26): 18001-13.  
<http://dx.doi.org/10.1039/D3RA02195E> PMID: 37323457
- [33] Lee HJ, Lee G, Jang NR, Yun JH, Song JY, Kim BS. Biological synthesis of copper nanoparticles using plant extract. *Nanotechnology* 2011; 1(1): 371-4.
- [34] Amaliyah S, Pangesti DP, Masruri M, Sabarudin A, Sumitro SB. Green synthesis and characterization of copper nanoparticles using *Piper retrofractum Vahl* extract as bioreductor and capping agent. *Heliyon* 2020; 6(8): e04636.  
<http://dx.doi.org/10.1016/j.heliyon.2020.e04636> PMID: 32793839
- [35] Babu Busi K, Palanivel M, Kanta Ghosh K, et al. The multifarious applications of copper nanoclusters in biosensing and bioimaging and their translational role in early disease detection. *Nanomaterials* 2022; 12(3): 301.  
<http://dx.doi.org/10.3390/nano12030301> PMID: 35159648
- [36] Sharma G, Sharma AR, Kurian M, Bhavesh R, Nam JS. Green synthesis of silver nanoparticle using *Myristica fragrans* (Nutmeg) seed extract and its biological activity. *Digest J Nanomater Biostruct* 2014; 9(1): 325-32.
- [37] Pak J, Khan TM, ul Mateen A, Khan B. Synthesis of copper nanoparticles via *Trigonella foenum graecum* seed extract for antibacterial response. *Anal Environ Chem* 2018; 19(2): 122-7.  
<http://dx.doi.org/10.21743/pjaec/2018.12.13>
- [38] Awad AM, Jalab R, Benamor A, et al. Adsorption of organic pollutants by nanomaterial-based adsorbents: An overview. *J Mol Liq* 2020; 301: 112335.  
<http://dx.doi.org/10.1016/j.molliq.2019.112335>
- [39] Ethaib S, Al-Qutaifa S, Al-Ansari N, Zubaidi SL. Function of nanomaterials in removing heavy metals for water and wastewater remediation: A review. *Environments* 2022; 9(10): 123.  
<http://dx.doi.org/10.3390/environments9100123>
- [40] Asghar N, Hussain A, Nguyen DA, et al. Advancement in nanomaterials for environmental pollutants remediation: A systematic review on bibliometrics analysis, material types, synthesis pathways, and related mechanisms. *J Nanobiotechnology* 2024; 22(1): 26.  
<http://dx.doi.org/10.1186/s12951-023-02151-3> PMID: 38200605
- [41] Sharma A, Pal K, Saini N, Kumar S, Bansal D, Mona S. Remediation of contaminants from wastewater using algal nanoparticles via green chemistry approach: An organized review. *Nanotechnology* 2023; 34(35): 352001-1.  
<http://dx.doi.org/10.1088/1361-6528/acd45a> PMID: 37167957

**DISCLAIMER:** The above article has been published, as is, ahead-of-print, to provide early visibility but is not the final version. Major publication processes like copyediting, proofing, typesetting and further review are still to be done and may lead to changes in the final published version, if it is eventually published. All legal disclaimers that apply to the final published article also apply to this ahead-of-print version.